analytical chemistry

pubs.acs.org/ac Article

Photoactivated Biosensing Process for Dictated ATP Detection in Single Living Cells

Zhijuan Duan, Liuxi Tan, Ruilin Duan, Mengxi Chen, Fan Xia, and Fujian Huang*

Cite This: *Anal. Chem.* 2021, 93, 11547−11556 Read Online

ACCESS | Metrics & More | Article Recommendations | Supporting Information

ABSTRACT: The subcellular distribution of adenosine 5′-triphosphate (ATP) and the concentration of ATP in living cells dynamically fluctuate with time during different cell cycles. The dictated activation of the biosensing process in living cells enables the spatiotemporal target detection in single living cells. Herein, a kind of *o*-nitrobenzylphosphate ester hairpin nucleic acid was introduced as a photoresponsive DNA probe for light-activated ATP detection in single living cells. Two methods to spatiotemporally activate the probe in single living cells were discussed. One method was the usage of the micrometer-sized optical fiber (about 5 μm) to guide the UV light (λ = 365 nm) to selectively activate the photoresponsive DNA probe in single living cells. The second method involved a two-photon laser confocal scanning microscope to selectively irradiate the photoresponsive DNA probes confined in single living cells via two-photon irradiation (λ = 740 nm). ATP aptamer integrated in the activated DNA probes selectively interacted with the target ATP, resulting in dictated signal generation. Furthermore, the photoactivated biosensing process enables dictated dual-model ATP detection in single living cells with "Signal-ON" fluorescence signal and "Signal-OFF" electrochemical signal outputs. The developed photoactivated biosensor for dictated ATP detection with high spatiotemporal resolution in single living cells at a desired time and desired place suggests the possibility to monitor biomarkers during different cell cycles.

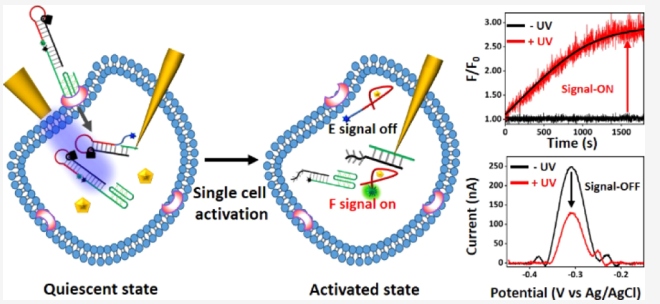

Over the past decades, biosensing techniques have been widely used in biomedicine, clinical diagnostics, environmental monitoring, and food safety.[1,2] Various biosensors have been developed for the detection of different types of analytes (such as small molecules, enzymes, and protein), including fluorescence,[3] electrochemistry,[4] colorimetric,[5] and chemiluminescence.[6] In particular, the biosensing process in single living cells allows the detection of cellular contents in single living cells and the monitoring of contents fluctuating with time in different cell cycles, thus providing important information for the course of the disease.[7] There are two types of biosensors: biosensors with a target recognition unit (target probe) and biosensors without a target recognition unit. Biosensors with a target recognition unit, which can selectively interact with the target, are desirable for the specific detection of target molecules. However, most of the current biosensors with a target recognition unit are "passive-type", which means that the target probes are "always active" and the target could interact with the probes directly.[8,9] This biosensing process is hard to control and may result in undesired signal generation and the target probe consumption during the process of probes reaching the dictated detection position. In principle, an "activable-type" biosensor would avoid this defect. In the biosensing process of the "activable-type" biosensor, the probe was kept inert until it was selectively activated at a desired time point and position. Thus, in the "activable-type" biosensing process, the dictated activation of the probes is possible, which enables the spatiotemporal detection of the target in single living cells.

To selectively activate the probes, remote and benign light control is a promising stimulus. Particularly, photoresponsive nucleic acids that include the *o*-nitrobenzylphosphate ester group as photocleavable protecting groups (PC-linker) were reported.[10] Upon irradiation, the photocleavable linker was cleaved to form an exposing toehold, which is used as an initiator to induce the strand displacement reaction.[11] Moreover, the activity of the photoresponsive system can be adjusted by the parameters including wavelength, exposure time, and light power.[12] Therefore, it is easy to achieve the dictated activation of the sensors and determine where and when to execute their activity in living systems with light irradiation.[13−15] Photoresponsive nucleic acids are widely used in biosensing,[16−18] photolithography,[19−22] DNA logical gate,[23] and other aspects.[24,25]

Received: May 14, 2021
Accepted: July 28, 2021
Published: August 10, 2021

Adenosine 5′-triphosphate (ATP) plays an important role in many biological processes.[26] ATP is the energy storage molecule and plays an important role in the metabolism and signaling process. In addition, the abnormal concentration of ATP is associated with many diseases.[27,28] For example, the excessive production of ATP is related with malignant tumor, cardiovascular diseases, Alzheimer's, and Parkinson's.[29] Also, ATP is used as an indicator for cellular viability and injury.[30] Therefore, the detection of ATP at the subcellular level is very important for the study of energy metabolism. A variety of strategies have been put up for ATP detection in cells.[31] For example, Tian et al.[32] developed a single two-photon fluorescence-lifetime-based probe, which provided a method for ATP and H_2O_2 imaging and detection in the mitochondria in two separated channels without crosstalk. Lu et al.[33] reported a photocleavable linker with DQAsomes to monitor ATP in the mitochondria in living cells. Nowadays, the analysis of ATP in single cells was brought up. Qi et al.[34] fabricated an electrochemical nanoelectrode to monitor ATP fluctuation in the mitochondria at the subcellular level. Jin et al.[35] used a functional glass nanopipette assembled with ATP-responsive gold nanoparticles to analyze the ATP concentration change in single normal cells and cancer cells during apoptosis.

Herein, we constructed a photoactivated biosensor by using a photoresponsive hairpin DNA modified with the PC-linker as probes for dictated ATP detection in single living cells with high spatiotemporal resolution. The photoactivatable DNA probe complex was modified with aptamer AS1411, which facilitated the probe to internalize into MCF-7 cancer cells via ligand-induced endocytosis.[36,37] The ATP aptamer in the DNA probe complex was activated in single living cells via UV irradiation (λ = 365 nm, guided by a micrometer-sized optical fiber) or two-photon irradiation (λ = 740 nm) controlled by confocal laser microscopy. The activated ATP aptamer could bind with ATP to generate a "Signal-ON" fluorescence signal in the cytoplasm, while the electrochemical signal was generated by a nanoelectrode inserting into the cell without a visible morphological change. The electrochemical photoactivatable hairpin DNA probe was immobilized on a nanoelectrode by the Au−S bond. At the initiation of the system, a significant electrochemical signal was obtained because of the redox-active groups MB approaching the surface of Au. Upon the irradiation of 365 nm UV light by the optical fiber, the electrochemical photoactivatable hairpin probe was cleaved, binding with ATP and releasing the strand modified with MB to generate a "Signal-OFF" electrochemical signal in the certain position of the cell. Thus, the photocontrollable biosensor for ATP detection can get a dual-signal fluorescence signal and electrochemical signal with high spatiotemporal resolution at a desired place and desired time.

EXPERIMENTAL SECTION

Materials. Ultrapure water with 18.2 mΩ cm was used in all experiments. All DNA oligonucleotide sequences used were purchased from Sangon Biotechnology Co., Ltd. (Shanghai, China) and purified by HPLC, and the detailed DNA sequences are shown in Supporting Information, Table S1. Tris(2-carboxyethyl)phosphine hydrochloride (TCEP), 6-mercapto-1-hexanol, Hochest 33258, and $CaCl_2$ were purchased from Sigma-Aldrich. Oligomycin was purchased from Sangon Biotechnology Co., Ltd. (Shanghai, China). Calcein-AM and propidium iodide (PI) were supplied by Yeasen Biotech Co., Ltd. (Shanghai, China). The buffer used in the experiment includes 20 mM Tris-HCl, 150 mM NaCl, and 5 mM $MgCl_2$ (pH = 7.5). A nanoelectrode with about 200 nm tip diameter was purchased from Jiangsu Rayme Biotechnology Co., Ltd. (Jiangsu, China). The outside of the nanoelectrode tip is coated with an Au layer.

Electrophoresis Experiment. The PF-Alex488/CP_F-Dabcyl complex was heated to 95 °C for 5 min and then cooled to room temperature for 3 h before use. Then, the samples were treated under different conditions: in the presence of ATP (5 mM), under UV irradiation, and both in the presence of ATP and UV irradiation. The gel was run in 12% PAGE gel with 1× TBE buffer at 100 V constant voltage and 25 °C for 1.5 h. The gel was stained with GelRed (Biotium) for 20 min to image the DNA position by using the Tanon imaging system (Tanon 5200 Multi).

Fluorescence Measurements in a Buffer Solution. The fluorescence intensity in the buffer solution was measured by an FS5 spectrofluorometer (Edinburgh Instruments). The emission spectra were recorded from 500 to 650 nm with an excitation wavelength of 495 nm. The performance of the strategy was evaluated by the intensity at 535 nm. 50 μL of solution containing a 100 nM PF-Alex488/CP_F-Dabcyl complex was used in the experiment. Also, 365 nm UV light was used to irradiate the reaction in the presence of 5 mM ATP, and the PF-Alex488/CP_F-Dabcyl complex was hybridized in a ratio of 1:1.5 in the fluorescence measurement. For fluorescence in droplet, 5 μL of Tris-buffer, consisting of a 500 nM PF-Alex488/CP_F-Dabcyl probe complex and 5 mM ATP, was exposed to UV light, and fluorescence was collected by using a single-cell analyzer (Jiangsu Rayme Biotechnology Co., Ltd., China) with a photomultiplier tube (PMT) after every 30 s of UV irradiation.

Electrochemistry Measurements in a Buffer Solution. The gold electrode surface was polished and cleaned according to the previously published protocol. The freshly washed gold electrode was modified with a 5 μL solution containing a 1 μM PE-MB/CP_E complex and 100 μM TCEP and incubated overnight at 4 °C. Then, the gold electrode was blocked by 2 mM 6-mercapto-1-hexanol. Then, the modified electrode was irradiated by UV light to initiate the reaction by adding 5 mM ATP. Electrochemical tests were performed including square wave voltammetry (SWV) and cyclic voltammetry (CV) to measure the electrochemical changes on the electrode surface. The frequency was set as 80 Hz.

Cell Culture. MCF-7 cell was grown in the Dulbecco's modified Eagle's medium with 10% fetal bovine serum (Gibco) and 0.5 mg/mL penicillin−streptomycin at 37 °C in 5% CO_2. The cells were incubated with different probes (CP_F-TAMRA, PF-Alex488, PF-Alex488/CP_F-Dabcyl, and PF-Alex488/CP_F-TAMRA-Dabcyl, 500 nM) at 37 °C in 5% CO_2 for 6 h. The confocal images were taken on a Zeiss LSM 880 with a 63× oil-immersion objective. $CaCl_2$ (5 μM, Sigma) and oligomycin (10 mM, Sigma) were used to upregulate or downregulate the concentration of ATP, respectively, in the MCF-7 cell.

Fluorescence Measurements in Single Living Cells. MCF-7 cells were incubated with the 500 nM PF-Alex488/CP_F-Dabcyl probe complex for 6 h at 37 °C in 5% CO_2. An optical fiber was used to guide the 365 nm UV light or two-photon irradiation with 740 nm light to a certain cell to photoactivate the PC linker, and the fluorescence intensity of the cell was collected by a single-cell analyzer (Jiangsu Rayme Biotechnology Co., Ltd., China) with PMT. The confocal images were taken by a Zeiss LSM 880 with a 63× oil-immersion objective. Selective two-photon irradiation of single living cells with 740 nm light

https://doi.org/10.1021/acs.analchem.1c02049
Anal. Chem. 2021, 93, 11547−11556

Scheme 1. (a) Principle of Photoactivated Probes for the "Signal-ON" Fluorescent Signal and "Signal-OFF" Electrochemical Signal of ATP Detection in a Single Cell, Activated by 365 nm UV Light Guided by the Optical Fiber

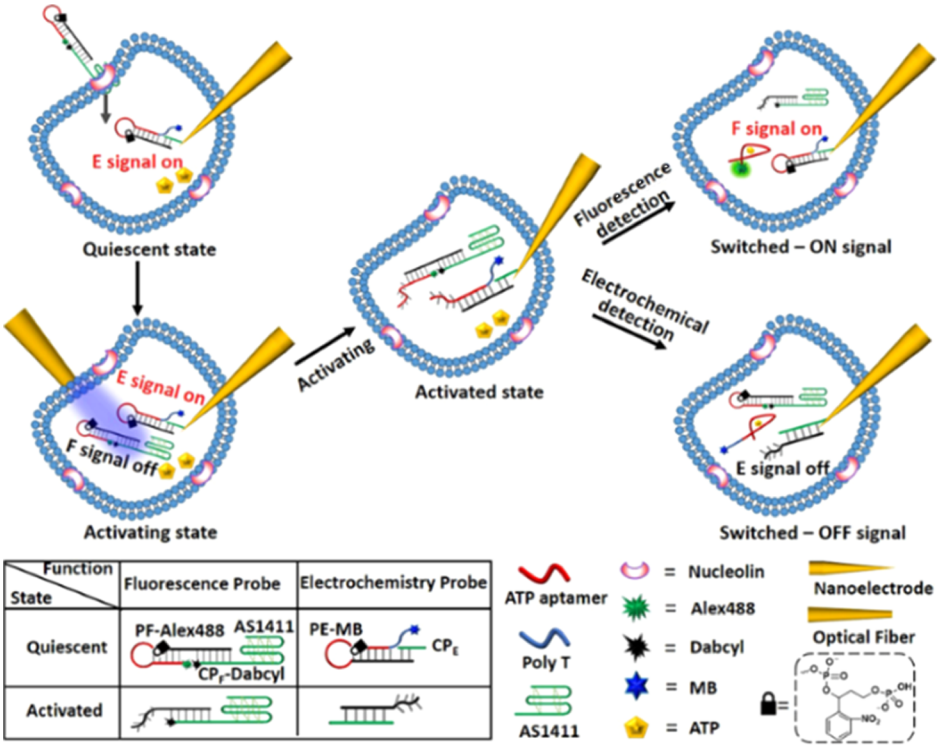

was achieved by using Zeiss LSM 880 confocal laser microscopy equipped femtosecond laser.

Electrochemical Measurements in Single Living Cells. A nanoelectrode was used to measure the electrochemical signal in single living cells. The nanoelectrode tip surface was modified with a DNA probe via the Au−S bond. The nanoelectrode tip was dipped into a 200 μL solution containing 1 μM PE-MB/CP$_E$ and 100 μM TCEP and incubated overnight at 4 °C. Subsequently, the modified nanoelectrode tip surface was blocked by 2 mM 6-mercapto-1-hexanol. Modified nanoelectrodes were tested via SWV in a blank solution before electrochemical measurements in single living cells, and nanoelectrodes were chosen from the same current signal level to control the effective surface area of the nanoelectrode. The working principle and setup of the single living cell detection system are shown in our previous work, Scheme S1.[13] Then, the nanoelectrode penetrated the single MCF-7 cell, irradiated by the UV light guided by the optical fiber. Electrochemical tests were performed including SWV and CV to measure the electrochemical changes on the electrode surface. The frequency was set as 500 Hz.

Upregulation and Downregulation of ATP in MCF-7 Cells. The upregulation of ATP in MCF-7 cells was stimulated by 10 mM oligomycin for 4 h and incubated with the probe PF-Alex488/CP$_F$-TAMRA-Dabcyl for 6 h. Also, the downregulation of ATP in MCF-7 cells was stimulated by 5 μM $CaCl_2$ for 4 h and incubated with the probe PF-Alex488/CP$_F$-TAMRA-Dabcyl for 6 h.

MCF-7 Cells Incubated with Nuclear Dye Hochest 33258. MCF-7 was incubated with probe PF-Alex488/CP$_F$-TAMRA for 6 h, followed by the incubation with 10 μM Hochest 33258 for 30 min.

MCF-7 Cells Incubated with Calcein-AM and PI. MCF-7 was incubated with 4 μM Calcein-AM (a commercially living cell probe) and 4 μM PI (a commercially dead cell probe) to verify the viability of the cell for 20 min. The cells with a yellow rectangle were the cells inserted by the nanoelectrode.

RESULTS AND DISCUSSION

Principle of the Photoactivated Biosensing Process for Dictated ATP Detection in Single Living Cells. As illustrated in Scheme 1, the photoresponsive DNA probe complex is composed of two parts: the carrier probe (CP$_F$-Dabcyl) and the photoresponsive target identification unit (PF-Alex488). The carrier probe is modified with a fluorescence quencher (Dabcyl) at its 3′ end and features an aptamer (AS1411) with a single-strand tail, which can specifically interact with nucleolin and be internalized into the cytoplasm. The photoresponsive target identification unit is modified with a fluorophore (Alex488) at its 5′ end and is linked by an *o*-nitrobenzyl photocleavable linker (PC-linker). It is a photoactivatable hairpin DNA with a protected ATP aptamer sequence and a single-strand tail (detailed sequences are shown in Table S1). The single-strand tail of CP$_F$-Dabcyl can hybridize with the single-strand tail of PF-Alex488, forming a PF-Alex488/CP$_F$-Dabcyl probe complex with quenched fluorescence. This probe complex can be internalized into the cytoplasm, and the protected ATP aptamer in the probe complex will remain in the quiescent state until activated by UV irradiation, which, in turn, interacted with ATP in living cells, finally releasing the "Signal-ON" Alex488 fluorescence signal.

Still another photoactivatable DNA probe was designed for dictated ATP detection with electrochemical signal generation. In this system, a thiol-modified DNA capture probe (CP$_E$) is immobilized on the surface of a nanoelectrode tip through the Au−S bond. The methylene blue (MB)-modified photoactivatable target identification unit (PE-MB) then hybridizes with the preimmobilized CP$_E$ (detailed sequences are shown in

https://doi.org/10.1021/acs.analchem.1c02049
Anal. Chem. 2021, 93, 11547−11556

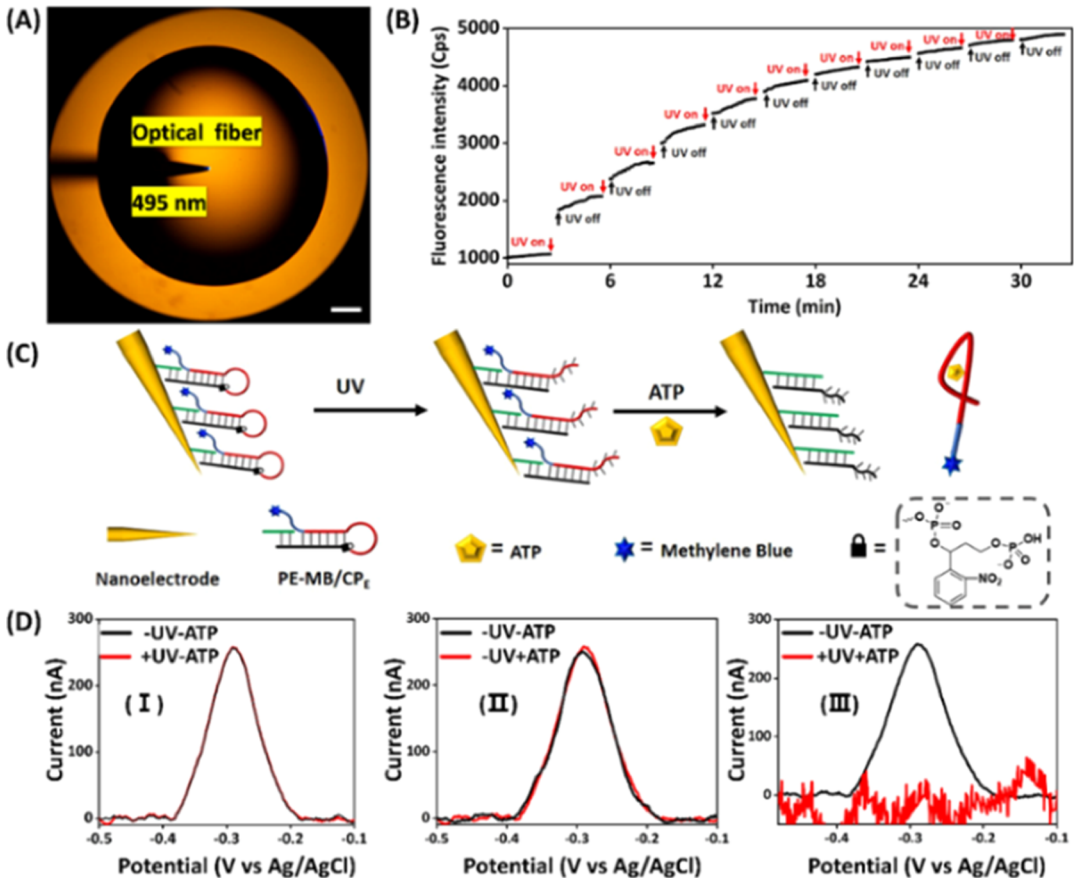

Figure 1. Signal of ATP detection in the aqueous solution with a single-cell analyzer. (A) Photograph of the droplet with the guidance of the optical fiber, and the scale bar is 50 μm. (B) Fluorescence data of the droplet collected by PMT. (C) Principle of electrochemical signal with the nanoelectrode. (D) SWV signal with the nanoelectrode under different conditions: (I) under the irradiation of UV light, (II) in the presence of ATP, and (III) both in the presence of UV light and ATP. The test condition was as follows: init E (V) = −0.5, final E (V) = 0, incr E (V) = −0.001, amplitude (V) = 0.05, frequency (Hz) = 500, quiet time (s) = 2, and sensitivity (A/V) = 1×10^{-6}.

Table S2). Hybridization causes the MB to be close to the surface of the nanoelectrode tip, allowing the modified nanoelectrode to be inserted into a single living cell at desired positions using a three-axis micromanipulation system to deliver PE-MB/CP$_E$. A polyT (10 T bases) sequence is designed at the 5′-end of the PE-MB to bring the MB close to the nanoelectrode surface for the generation of the MB signal. Upon UV irradiation in single living cells, the protected ATP aptamer in PE-MB is activated to initiate the specific binding with ATP in living cells. After binding with ATP, the MB-modified DNA strand is released from the tip surface, resulting in a decrease in the electrochemical signal. Therefore, a photoactivated biosensor with the functioned PE-MB/CP$_E$ electrochemical probe complex has been put forward for dictated ATP detection with the "Signal-OFF" electrochemical signal in single living cells.

Dictated ATP Detection Performance in Aqueous Solution. Photoactivated biosensor for dictated ATP detection was first verified in an aqueous solution. To verify the principle of the photoactivated biosensing process (Figure S1A), the whole process was verified under different conditions by fluorescence spectra (Figure S1B) and native PAGE gel electrophoresis (Figure S1D). The fluorescence intensity increased with the extension of the UV irradiation time, and the fluorescence intensity was saturated nearly after 5 min (Figure S1C). It can be seen that the fluorescence intensity increased with the increase of ATP concentration from 0 to 7 mM (Figure S1E). It had a good linear relationship between the fluorescence and ATP concentration in the range of 0−1 mM, as shown in Figure S1F, which could match the ATP concentration in living cells.[38] Moreover, the system had a good specificity for ATP detection (Figure S1H).

In addition to obtaining the fluorescence signal, a photoactivated electrochemical DNA probe complex was designed (Figure S2A) to get the "Signal-OFF" electrochemical signal. The performance of the photoactivatable DNA probe for electrochemical signal generation was tested using a disk electrode. It can be seen that the signal of SWV and CV did not change or changed slightly with UV light or in the presence of ATP compared with the electrochemical signal decreased a lot when irradiated by UV light in the presence of ATP (Figure S2B). The electrochemical signal of SWV E/E_0 was used to evaluate the performance of the PE-MB/CP$_E$ complex. The electrochemical signal E/E_0 decreased with the concentration of ATP from 0 to 10 mM (Figure S2C). A good linear relationship between the electrochemical signal and the concentration of ATP from 0 to 1 mM is observed in Figure S2D.

Next, the performance of the fluorescence collection system and nanoelectrode in the single living cells analysis system was investigated by using these photocontrollable fluorescence and electrochemical DNA probe complex. The optical fiber/nanofiber coupled with 495 nm external excitation light was inserted into a 5 μL droplet containing the photoactivatable PF-Alex488/CP$_F$-Dabcyl probe complex and 5 mM ATP at a

https://doi.org/10.1021/acs.analchem.1c02049
Anal. Chem. 2021, 93, 11547−11556

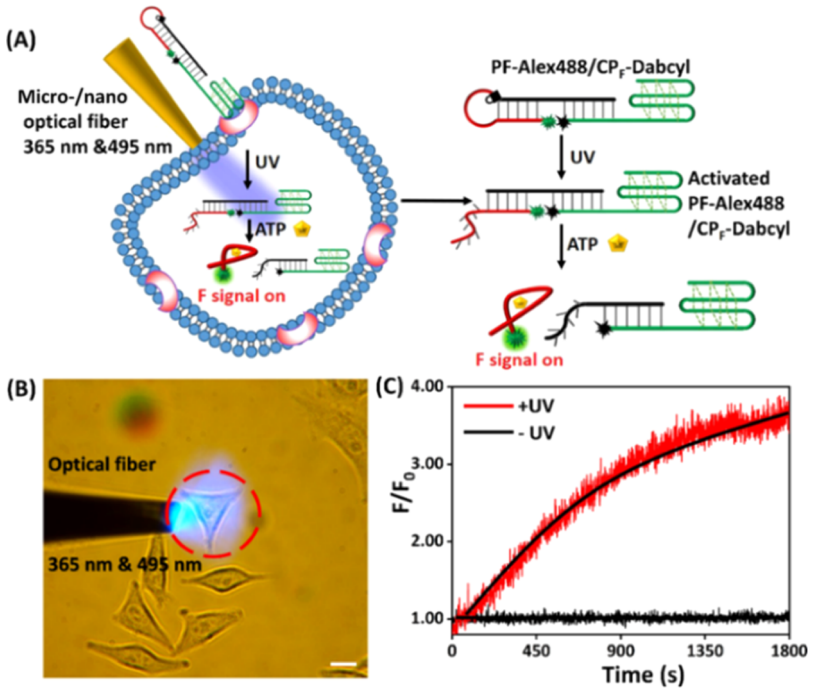

Figure 2. Fluorescence signal of a single cell irradiated by 365 nm UV light with the optical fiber. (A) Scheme of the photoactivated displacement reaction in a single cell for ATP detection. (B) Photograph of the optical fiber under the guidance of 365 and 495 nm light to the cell, and the scale bar is 5 μm. (C) Fluorescence signal of a single cell with UV light irradiation and without UV light irradiation by the optical fiber with 365 nm UV light.

desired position (Figure 1A). As shown in Figure 1B, the droplet was exposed to UV light, and after 30 s of UV irradiation, fluorescence increased immediately and significantly. The fluorescence intensity reached a plateau after UV irradiation 10 times (30 s each irradiation for a total of 5 min of UV irradiation), representing a 4.5-fold increase in the fluorescence intensity over the initial value after 5 min of UV irradiation. These data indicated the efficient collection of the desired fluorescence signal by the fluorescence detection system. For the testing of the nanoelectrode performance, the surface of the nanoelectrode tip was modified with the PE-MB/CP$_E$ probe complex and blocked by 6-mercapto-1-hexanol (Figure 1C). The ATP aptamer in the DNA probe complex was activated by UV irradiation, which initiated the binding of the activated ATP aptamer with the target ATP and resulted in a significant decrease of the electrochemical signal (panel III, Figure 1D) compared with that in the absence of ATP (panel I, Figure 1D) or without UV irradiation (panel II, Figure 1D).

Dictated ATP Detection with the "Signal-ON" Fluorescence Signal in Single Living Cells. Both photoactivated DNA probe complex and signal collection systems were shown to work as expected. Therefore, we next tested the ability of the photoactivated DNA probe complex PF-Alex488/CP$_F$-Dabcyl together with the integrated fluorescent signal collection system to detect ATP in a single MCF-7 cancer cell with a "Signal-ON" fluorescent signal output. First, it was necessary to confirm that the probe complex could be internalized by the MCF-7 cancer cell and be photocontrollably activated, as expected. To make this determination, PF labeled with Alex488 (PF-Alex488) and CP$_F$ labeled with TAMRA (CP$_F$-TAMRA) were used to assess the internalization ability of aptamer AS1411 (Figure S3). Then, we used PF-Alex488/CP$_F$-TAMRA-Dabcyl to evaluate the photoactivated process in living cells. Once the probe complex was internalized into the cytoplasm of MCF-7 cells, the probe's photoactivation process was initiated by UV irradiation to, in turn, trigger the displacement reaction in the MCF-7 cytoplasm. Without UV irradiation, the probe complex PF-Alex488/CP$_F$-TAMRA-Dabcyl remained inert, and no reaction could proceed (Figure S4A,B). Oligomycin and calcium ions were used to downregulate and upregulate the expression level of ATP in the cytoplasm of MCF-7 cells (Figure S4C,D), which corresponded to the references.[39,40] The corresponding average optical density (AOD) under different conditions was obtained by NIH Image software in Figure S5. These results demonstrated that the probe complex PF-Alex488/CP$_F$-TAMRA-Dabcyl worked as we expected. DNA probe PF-Alex488/CP$_F$-TAMRA was incubated with cells for 6 h to make the DNA probes go inside the cytoplasm, which was verified by using the Hoechst 33258 dye to stain the cell nucleus, as shown in Figure S6.

After performing these preliminary experiments, ATP sensing in single MCF-7 cells was further performed using the optical fiber/nanofiber to selectively activate the probe in a single MCF-7 cell. In the experiment, the probe complex PF-Alex488/CP$_F$-Dabcyl was incubated with MCF-7 cells for 6 h, and then, the optical fiber approached the certain cell's cytomembrane under the guidance of 365 nm UV light and the excitation wavelength of 495 nm with a three-axis micromanipulation system (Figure 2A,B). Upon the irradiation of 365 nm UV light, the complex PF-Alex488/CP$_F$-Dabcyl was activated and binded with ATP inside the cell to release to the cytoplasm. External light of 495 nm was used as the excitation light to obtain the PF-Alex488 fluorescence signal collected by PMT. After the probe complex PF-Alex488/CP$_F$-Dabcyl reacted for 30 min in the cells, the fluorescence intensity was nearly not changed without UV light irradiation. On the contrary, the fluorescence intensity with UV light irradiation increased nearly 3.6-fold higher than the fluorescence intensity without UV irradiation during the reaction time (Figure 2C). The 365 nm UV light did not affect the viability of the cells (Figure S7). These results showed that our designed DNA probe could be used for photoactivated ATP

https://doi.org/10.1021/acs.analchem.1c02049
Anal. Chem. 2021, 93, 11547−11556

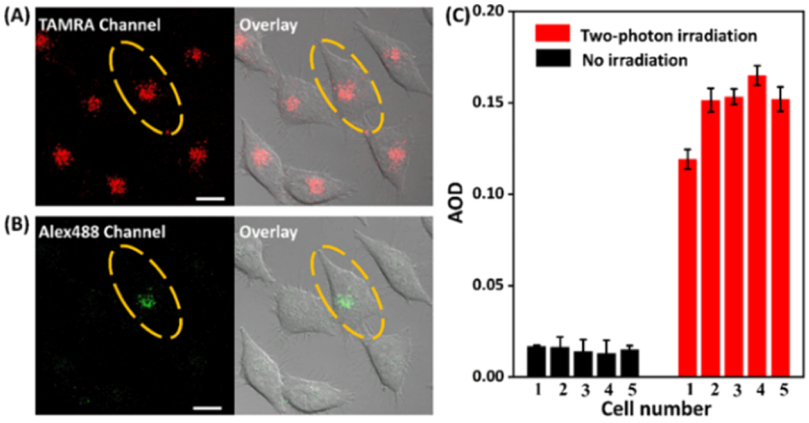

Figure 3. Fluorescence signal of a single cell irradiated by two-photon. (A) Confocal microscopy images of MCF-7 cells treated with the PF-Alex488/CP_F-Dabcyl-TAMRA complex with the irradiation of two-photon in the TAMRA channel; the cell circled in yellow ellipse is irradiated by two-photon. (B) MCF-7 cells irradiated by two-photon in the Alex488 channel; the cell circled in yellow ellipse is irradiated by two-photon. (C) AOD of a single cell with irradiation and without irradiation by two-photon irradiation with 740 nm light in five different cells. The scale bar is 20 μm in the above experiments.

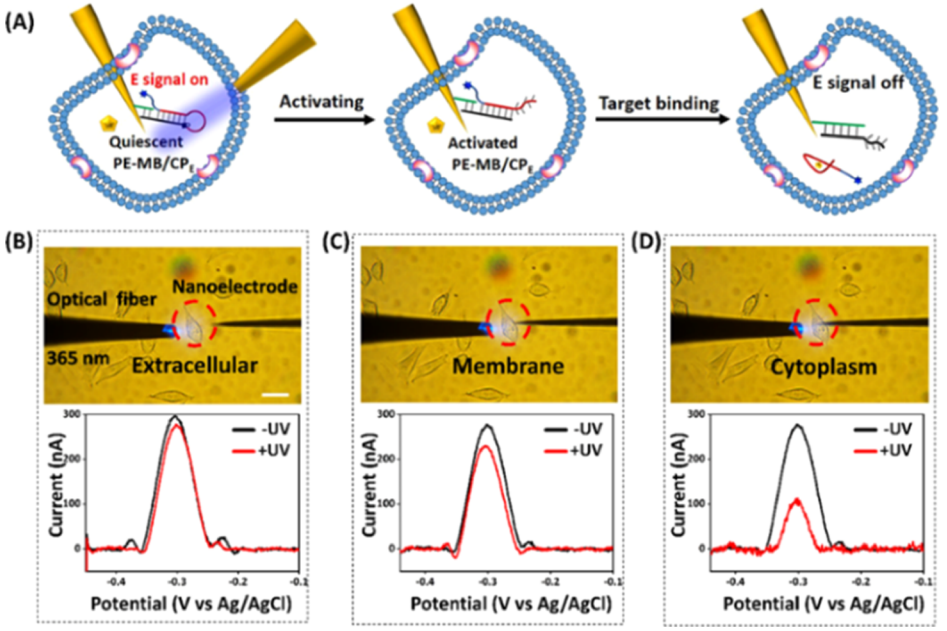

Figure 4. Electrochemical signal in a single cell with a nanoelectrode for ATP detection. (A) Illustration of ATP detection with a nanoelectrode in a single cell. Electrochemical signal of ATP detection in different positions of the cell: (B) extracellular, (C) membrane, and (D) cytoplasm; the scale bar is 10 μm in the above experiments. The test condition was as follows: init E (V) = −0.5, final E (V) = 0, incr E (V) = 0.001, amplitude (V) = 0.05, frequency (Hz) = 800, quiet time (s) = 2, and sensitivity (A/V) = 1×10^{-6}.

sensing in a single cell. Moreover, the probes could be used to discriminate among cells with different levels of ATP expression via the fluorescent method.

Two-photon is a good choice for efficiently cleaving the photolabile groups.[41−43] The maximum absorption of the caging group is 365 nm, which can be excited by light at around twice of the maximum absorption of 730 nm. Two-photon absorption only occurs at the focus of a laser. Thus, we chose two-photon as another irradiated way to photoactivate the certain single cell, precisely. Confocal microscopy was used to more intuitively observe the single living cell selectively, irradiated by two-photon light. MCF-7 cells were incubated with the PF-Alex488/CP_F-TAMRA-Dabcyl probe complex. After 6 h of incubation, the single living cell was marked and selectively irradiated by two-photon light and imaged with confocal microscopy. Resulting images showed that the TAMRA signal could be observed in all cells, indicating that the PF-Alex488/CP_F-TAMRA-Dabcyl probe complex had been internalized in all cells (Figure 3A). In contrast, the PF-Alex488 signal could only be observed in the activated single cell circled by a yellow ellipse, while no signal was emitted from the surrounding cells. Because the probe in cells which had not undergone UV irradiation remained quiescent, it could not initiate the displacement reaction, even in the presence of ATP (Figure 3B). Five different cells were studied in parallel to explore the reproducibility of the two-photon irradiation method. Evaluated by AOD of the PF-Alex488 signal, the cells had a low PF-Alex488 signal value without irradiation, while the cells with two-photon irradiation had a higher PF-Alex488 signal value (Figure 3C). These results

https://doi.org/10.1021/acs.analchem.1c02049
Anal. Chem. 2021, 93, 11547−11556

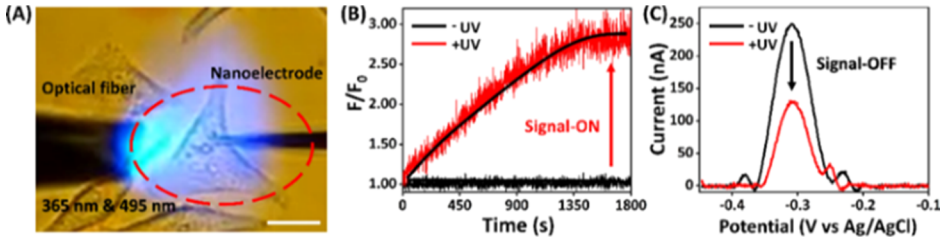

Figure 5. Dual-modal ATP detection in single living cells. (A) Photograph of ATP detection with a nanoelectrode inserted into the single cell under the guidance of the optical fiber with 365 and 495 nm light, and the scale bar is 5 μm. (B) Fluorescence signal of ATP detection in a single cell. (C) Electrochemical signal of ATP detection in a single cell. The test condition was as follows: init E (V) = −0.5, final E (V) = 0, incr E (V) = 0.001, amplitude (V) = 0.05, frequency (Hz) = 800, quiet time (s) = 2, and sensitivity (A/V) = 1×10^{-6}.

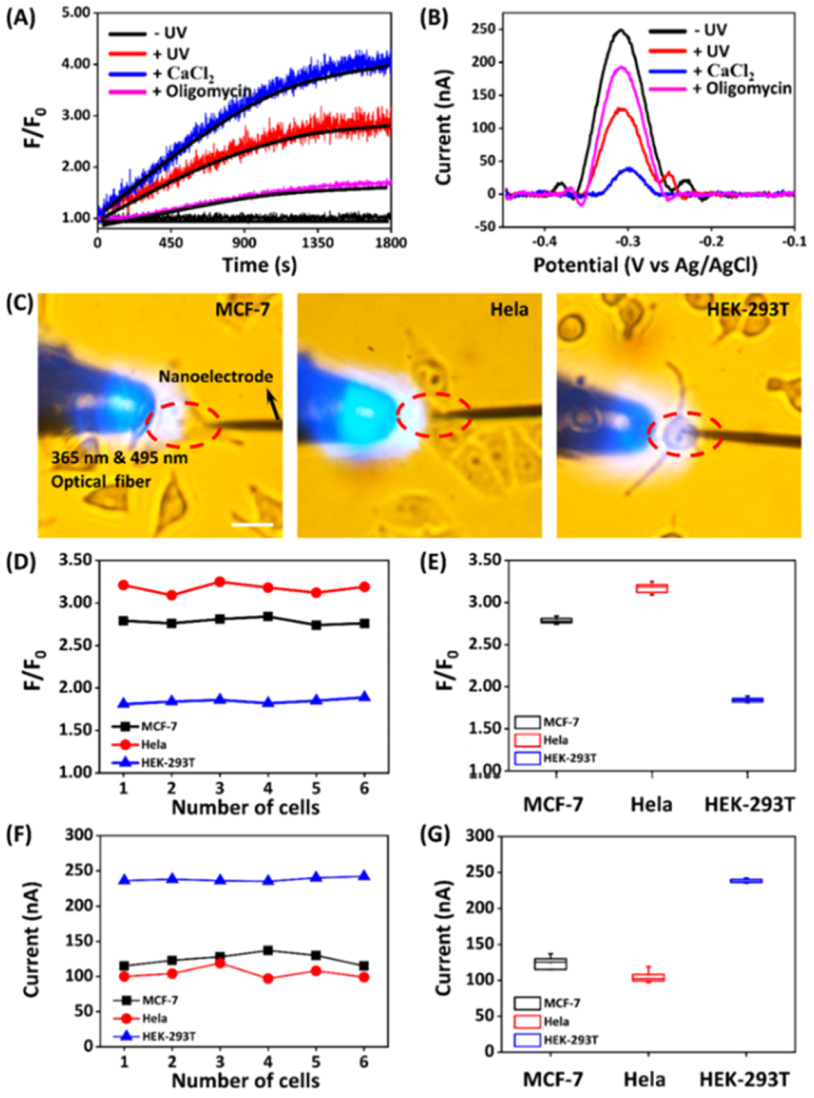

Figure 6. Signal of ATP detection under different situations and in different cell lines. (A) Fluorescence signal of MCF-7 cells without UV, with UV, treatment with 5 μM $CaCl_2$, and treatment with 10 mM oligomycin. (B) Electrochemical signal of MCF-7 cells without UV, with UV, treatment with 5 μM $CaCl_2$, and treatment with 10 mM oligomycin. (C) Photograph of the nanoelectrode inserted into three different cell lines: MCF-7 cells, HeLa cells, and HEK293T cells. (D) Fluorescence signal for six cells from single-cell ATP detection for the three tested cell lines. (E) Comparison of the fluorescence signal for ATP detection in single MCF-7, HeLa, and HEK293T cells. (F) Electrochemical signal for six cells from single-cell ATP detection for the three tested cell lines. (G) Comparison of the electrochemical signal for ATP detection in single MCF-7, HeLa, and HEK293T cells. The scale bar is 5 μm.

proved that the probes could be precisely activated at the single-cell level without affecting the surrounding cells.

Dictated ATP Detection with the "Signal-OFF" Electrochemical Signal in Single Living Cells. As previously described, the photoactivated DNA probe, together with the integrated electrochemical signal collection system, can also work as expected in the buffer solution. Here, we further used the photoactivated DNA probe to detect ATP in single living

https://doi.org/10.1021/acs.analchem.1c02049
Anal. Chem. 2021, 93, 11547−11556

MCF-7 cells. The photoactivated DNA probe PE-MB/CP_E was immobilized on the tip of the nanoelectrode by the Au−S bond. The tip diameter of the nanoelectrode was 230 nm, and a scanning electron microscopy (SEM) image is shown in Figure S8. The nanoelectrode was sharp enough to insert the cell with minimal invasiveness, which was verified by confocal microscopy after staining with Calcein-AM and PI. Confocal images showed that MCF-7 cells exhibited green fluorescence, even the marked with yellow rectangular cells were inserted by the nanoelectrode (Figure S9). The nanoelectrode was inserted into a single living MCF-7 cell, and the optical fiber was used as the guide of 365 nm UV light, approaching the cytomembrane of the certain single MCF-7 cell (Figure 4A) (Video S1). The nanopipette was inserted into three different positions of the cell: extracellular, membrane, and cytoplasm. The SWV signal changed slightly in the extracellular cell (Figure 4B) and membrane (Figure 4C) with or without UV irradiation, indicating the low concentration level of ATP in the extracellular and membrane, while it had a significant drop inside the cytoplasm of the cell, indicating a high concentration level of ATP in the cytoplasm (Figure 4D). These results showed that our designed photoactivated electrochemical probe could be used to detect the concentration of ATP in different subcellular regions of a single MCF-7 cell.

Dual-Modal Signal Outputs for Dictated ATP Detection in Single Living Cells. For the practical use of ATP sensing, one target that presented different kinds of signal outputs could provide more faithful results than that with only one kind of signal output. Therefore, as a proof-of-concept, ATP sensing in a MCF-7 single cell with both "Signal-ON" fluorescence signal and "Signal-OFF" electrochemical signal outputs was demonstrated with the photoactivated DNA probe equipped with a dual signal. First, MCF-7 cells were incubated with the PF-Alex488/CP_F-Dabcyl probe complex. After incubation, the nanoelectrode immobilized with the photoactivated electrochemical probe PE-MB/CP_E was inserted into the selected single MCF-7 cell. Also, the optical fiber was approaching the cytomembrane of the selected single MCF-7 cell (Figure 5A). The optical fiber was around 5 μm, the corresponding light spot diameter was around 12 μm, and the diameter of the cell was around 10 μm. The diameter of the light spot is consistent with the cell size, which enables the selective irradiation in the single living cell level. With 365 nm UV light irradiation for 5 min, photoactivated probes PF-Alex488/CP_F-Dabcyl and PE-MB/CP_E were activated, which released the hidden toehold and initiated the displacement reaction in the presence of ATP of the single MCF-7 cell. After 30 min of reaction time, excited by 495 nm light, a "Signal-ON" fluorescence signal was obtained along with a "Signal-OFF" electrochemical signal. The fluorescence intensity with UV irradiation was 3-fold higher than the fluorescence intensity without UV irradiation, which was lower than that with only a fluorescence signal output (increased about 3.6-fold) (Figure 5B). At the same time, a decreased electrochemical signal by 49% was obtained, which was lower than that with only an electrochemical signal output (decreased about 58%) (Figure 5C). In the dual model, ATP would react with both photoactivated DNA probes in the cytoplasm of the single cell, and the photoactivated DNA probes on the surface of the nanoelectrode tip, in turn, generated both fluorescence and electrochemical signals. Thus, the dual model would tend to reduce the fluorescence/electrochemical signal to a lesser extent than that with only fluorescence/electrochemical signal output.

Monitoring ATP Fluctuation at a Subcellular Level under External Stimulus and Relative Concentration of ATP in Different Cell Lines. It has been reported that Ca^{2+} promotes ATP production by activating mitochondrial dehydrogenases. Moreover, oligomycin decreased the ATP concentration level by inhibiting oxidative phosphorylation. It can be concluded that the fluorescence intensity F/F_0 treated with Ca^{2+} was around 4.17, higher than treated with UV light 3.07. Inversely, the fluorescence intensity F/F_0 treated with oligomycin was about 1.75 lower than the sample treated with UV light 3.07 (Figure 6A). The electrochemical signal was 250.37 nA without UV irradiation. With UV irradiation, the electrochemical signal was 131.67 nA, higher than the electrochemical signal treated with Ca^{2+} (38.93 nA) and lower than the electrochemical signal treated with oligomycin (Figure 6B).

To prove the versatility of our method, we chose another cell line, human cervical cancer cell (HeLa) and human embryonic kidney 293T (HEK-293T), to obtain the fluorescence signal and electrochemical signal (Figure 6C). From Figure 6D,E, the fluorescence intensity F/F_0 in the MCF-7 cell was 2.80, 3.12 in the HeLa cell, and 1.84 in the HEK-293T cell. It can be seen that the fluorescence intensity F/F_0 from high to low was as follows: HeLa > MCF-7 > HEK-293T. Owing to the fluorescence probe was a "Signal-ON" sensor, which corresponded to the concentration of ATP in different cells from high to low: HeLa > MCF-7 > HEK-293T, while the electrochemical probe was a "Signal-OFF" probe. It can be seen from Figure 6F,G that the electrochemical signal in the MCF-7 cell was 121.77, 104.48 in the case of HeLa cell, and 241.79 nA in the HEK-293T cell. The electrochemical signal from high to low was as follows: HEK-293T > MCF-7 > HeLa. The result corresponded to the concentration of ATP from high to low: HeLa > MCF-7 > HEK-293T. The electrochemical result of the concentration of ATP in different cells was the same with the fluorescent result. Compared with cancerous MCF-7 cells and HeLa cells, noncancerous HEK-293T cells showed a lowest fluorescent signal and highest electrochemical signal, indicating a lowest intracellular ATP level. We could use this method to quantify the target in single cells to get more accurate results.

CONCLUSIONS

In summary, we have demonstrated a photoactivated biosensor to detect ATP in single cells at a desired place and desired time with the single living cell level spatiotemporal resolution. Photoactivated DNA probes were sophisticatedly designed with an *o*-nitrophenylphosphate ester modified with Alex488 fluorophore and redox-active groups MB to obtain the fluorescence signal and electrochemical signal. The fluorescence hairpin probe was inactivated at the quenched state, whereas the electrochemical probe was immobilized on the nanoelectrode tip. Irradiated by 365 nm UV light, the caged fluorescence hairpin probe was cleaved to get the "Signal-ON" fluorescence signal. Meanwhile, electrochemical probes were activated to release the DNA strand modified with MB to get the "Signal-OFF" electrochemical signal. Therefore, an ATP biosensor has been constructed, which could be inactivated or caged before reaching the cell and be activated or decaged upon the irradiation of light to detect ATP in single living cells. It is useful for monitoring the biomarkers during the biological process in single living cells. The subcellular spatial control by using our developed method could be achieved via designing a DNA sequence to target different subcellular organelles[25,44,45] in

https://doi.org/10.1021/acs.analchem.1c02049
Anal. Chem. 2021, 93, 11547−11556

a future study. Based on the reported literature studies,[45,46] our proposed principle may provide a strategy to monitor the time-dependent change of the intracellular molecular level. The developed multimode detection platforms by coupling the "Signal-ON" fluorescence signal and "Signal-OFF" electrochemical signal in single living cells are important to prevent "false-positive" or "false-negative" results that are often encountered in single "Signal-ON" or "Signal-OFF" transduction means.[47]

■ ASSOCIATED CONTENT

Supporting Information

The Supporting Information is available free of charge at https://pubs.acs.org/doi/10.1021/acs.analchem.1c02049.

DNA sequences in the fluorescence system and in the electrochemical system; fluorescence signal of ATP detection in the aqueous solution and electrochemical signal; confocal images of MCF-7 cells treated under different conditions; SEM image of the nanoelectrode tip; and viability of penetrated cells (PDF)

Nanoelectrode inserted into a single living MCF-7 cell (AVI)

■ AUTHOR INFORMATION

Corresponding Author

Fujian Huang − *State Key Laboratory of Biogeology and Environmental Geology, Engineering Research Center of Nano-Geomaterials of Ministry of Education, Faculty of Materials Science and Chemistry, China University of Geosciences, Wuhan 430074, China;* orcid.org/0000-0002-7777-1589; Email: huangfj@cug.edu.cn

Authors

Zhijuan Duan − *State Key Laboratory of Biogeology and Environmental Geology, Engineering Research Center of Nano-Geomaterials of Ministry of Education, Faculty of Materials Science and Chemistry, China University of Geosciences, Wuhan 430074, China*

Liuxi Tan − *State Key Laboratory of Biogeology and Environmental Geology, Engineering Research Center of Nano-Geomaterials of Ministry of Education, Faculty of Materials Science and Chemistry, China University of Geosciences, Wuhan 430074, China*

Ruilin Duan − *State Key Laboratory of Biogeology and Environmental Geology, Engineering Research Center of Nano-Geomaterials of Ministry of Education, Faculty of Materials Science and Chemistry, China University of Geosciences, Wuhan 430074, China*

Mengxi Chen − *State Key Laboratory of Biogeology and Environmental Geology, Engineering Research Center of Nano-Geomaterials of Ministry of Education, Faculty of Materials Science and Chemistry, China University of Geosciences, Wuhan 430074, China*

Fan Xia − *State Key Laboratory of Biogeology and Environmental Geology, Engineering Research Center of Nano-Geomaterials of Ministry of Education, Faculty of Materials Science and Chemistry, China University of Geosciences, Wuhan 430074, China;* orcid.org/0000-0001-7705-4638

Complete contact information is available at: https://pubs.acs.org/10.1021/acs.analchem.1c02049

Notes

The authors declare no competing financial interest.

■ ACKNOWLEDGMENTS

This work was supported by the National Natural Science Foundation of China (21974127, 22090050, and 21874121), the National Key Research and Development Program of China (2018YFE0206900), Hubei Provincial Natural Science Foundation of China (2020CFA037), and Zhejiang Provincial Natural Science Foundation of China under grant nos LD21B050001 and LY20B050001.

■ REFERENCES

(1) Li, Y.; Tian, C.; Liu, Z.; Jiang, W.; Mao, C. *Angew. Chem., Int. Ed.* **2015**, *54*, 5990−5993.
(2) Wang, Z.; Li, F.; Zhang, L.; Qian, J.; Cao, S. *Nanotechnology* **2020**, *31*, 455603.
(3) Jiang, Y. S.; Bhadra, S.; Li, B.; Ellington, A. D. *Angew. Chem., Int. Ed.* **2014**, *53*, 1845−1848.
(4) Lilienthal, S.; Shpilt, Z.; Wang, F.; Orbach, R.; Willner, I. *ACS Appl. Mater. Interfaces* **2015**, *7*, 8923−8931.
(5) Song, G.; Chen, C.; Ren, J.; Qu, X. *ACS Nano* **2009**, *3*, 1183−1189.
(6) Zhang, L.; Guo, S.; Zhu, J.; Zhou, Z.; Li, T.; Li, J.; Dong, S.; Wang, E. *Anal. Chem.* **2015**, *87*, 11295−11300.
(7) Zhu, Z.; Yang, C. J. *Acc. Chem. Res.* **2016**, *50*, 22−31.
(8) Li, H.; Dauphin-Ducharme, P.; Ortega, G.; Plaxco, K. W. *J. Am. Chem. Soc.* **2017**, *139*, 11207−11213.
(9) Li, H.; Arroyo-Currás, N.; Kang, D.; Ricci, F.; Plaxco, K. W. *J. Am. Chem. Soc.* **2016**, *138*, 15809−15812.
(10) Ordoukhanian, P.; Taylor, J.-S. *J. Am. Chem. Soc.* **1995**, *117*, 9570−9571.
(11) Huang, F.; You, M.; Han, D.; Xiong, X.; Liang, H.; Tan, W. *J. Am. Chem. Soc.* **2013**, *135*, 7967−7973.
(12) Huang, C.-H.; Park, Y. I.; Lin, H.-Y.; Pathania, D.; Park, K. S.; Avila-Wallace, M.; Castro, C. M.; Weissleder, R.; Lee, H. *ACS Nano* **2019**, *13*, 11698−11706.
(13) Huang, F.; Lin, M.; Duan, R.; Lou, X.; Xia, F.; Willner, I. *Nano Lett.* **2018**, *18*, 5116−5123.
(14) Huang, F.; Duan, R.; Zhou, Z.; Vázquez-González, M.; Xia, F.; Willner, I. *Chem. Sci.* **2020**, *11*, 5592−5600.
(15) Zhao, J.; Chu, H.; Zhao, Y.; Lu, Y.; Li, L. *J. Am. Chem. Soc.* **2019**, *141*, 7056−7062.
(16) Duan, R.; Li, T.; Duan, Z.; Huang, F.; Xia, F. *Anal. Chem.* **2020**, *92*, 5846−5854.
(17) Lin, M.; Yi, X.; Huang, F.; Ma, X.; Zuo, X.; Xia, F. *Anal. Chem.* **2019**, *91*, 2021−2027.
(18) Lin, M.; Yi, X.; Wan, H.; Zhang, J.; Huang, F.; Xia, F. *Anal. Chem.* **2020**, *92*, 9963−9970.
(19) Pardatscher, G.; Matthaeus, S. S.; Daube, S. S.; Bar Ziv, R. H.; Simmel, F. C. *Angew. Chem., Int. Ed.* **2018**, *57*, 4783−4786.
(20) Huang, F.; Zhang, J.; Li, T.; Duan, R.; Xia, F.; Willner, I. *Nano Lett.* **2019**, *19*, 618−625.
(21) Huang, F.; Zhou, X.; Yao, D.; Xiao, S.; Liang, H. *Small* **2015**, *11*, 5800−5806.
(22) Huang, F.; Xu, H.; Tan, W.; Liang, H. *ACS Nano* **2014**, *8*, 6849−6855.
(23) Chen, S.; Xu, Z.; Yang, W.; Lin, X.; Li, J.; Li, J.; Yang, H. *Angew. Chem., Int. Ed.* **2019**, *58*, 18186−18190.
(24) Huang, F.; Liao, W.-C.; Sohn, Y. S.; Nechushtai, R.; Lu, C.-H.; Willner, I. *J. Am. Chem. Soc.* **2016**, *138*, 8936−8945.
(25) Chu, H.; Zhao, J.; Mi, Y.; Di, Z.; Li, L. *Nat. Commun.* **2019**, *10*, 2839.
(26) Green, D. R.; Kroemer, G. *Science* **2004**, *305*, 626−629.
(27) Wallace, D. C. *Science* **1999**, *283*, 1482−1488.
(28) Gourine, A. V.; Llaudet, E.; Dale, N.; Spyer, K. M. *Nature* **2005**, *436*, 108−111.

(29) Finkel, T.; Serrano, M.; Blasco, M. A. *Nature* **2007**, *448*, 767−774.
(30) Weiss, J. N.; Lamp, S. T. *J. Gen. Physiol.* **1989**, *94*, 911−935.
(31) Zhao, J.; Gao, J.; Xue, W.; Di, Z.; Xing, H.; Lu, Y.; Li, L. *J. Am. Chem. Soc.* **2018**, *140*, 578−581.
(32) Wu, Z.; Liu, M.; Liu, Z.; Tian, Y. *J. Am. Chem. Soc.* **2020**, *142*, 7532−7541.
(33) Hong, S.; Zhang, X.; Lake, R. J.; Pawel, G. T.; Guo, Z.; Pei, R.; Lu, Y. *Chem. Sci.* **2020**, *11*, 713−720.
(34) Zheng, J.; Li, X.; Wang, K.; Song, J.; Qi, H. *Anal. Chem.* **2020**, *92*, 10940−10945.
(35) Wang, D.; Qi, G.; Zhou, Y.; Zhang, Y.; Wang, B.; Hu, P.; Jin, Y. *Chem. Commun.* **2020**, *56*, 1561−1564.
(36) Cao, Z.; Tong, R.; Mishra, A.; Xu, W.; Wong, G. C. L.; Cheng, J.; Lu, Y. *Angew. Chem., Int. Ed.* **2009**, *48*, 6494−6498.
(37) Chen, W.-H.; Yu, X.; Liao, W.-C.; Sohn, Y. S.; Cecconello, A.; Kozell, A.; Nechushtai, R.; Willner, I. *Adv. Funct. Mater.* **2017**, *27*, 1702102.
(38) Arai, S.; Kriszt, R.; Harada, K.; Looi, L.-S.; Matsuda, S.; Wongso, D.; Suo, S.; Ishiura, S.; Tseng, Y.-H.; Raghunath, M.; Ito, T.; Tsuboi, T.; Kitaguchi, T. *Angew. Chem., Int. Ed.* **2018**, *57*, 10873−10878.
(39) Zheng, X.; Peng, R.; Jiang, X.; Wang, Y.; Xu, S.; Ke, G.; Fu, T.; Liu, Q.; Huan, S.; Zhang, X. *Anal. Chem.* **2017**, *89*, 10941−10947.
(40) Gong, Y.; Sohn, H.; Xue, L.; Firestone, G. L.; Bjeldanes, L. F. *Cancer Res.* **2006**, *66*, 4880−4887.
(41) Tam, D. Y.; Dai, Z.; Chan, M. S.; Liu, L. S.; Cheung, M. C.; Bolze, F.; Tin, C.; Lo, P. K. *Angew. Chem., Int. Ed.* **2016**, *55*, 164−168.
(42) Lunzer, M.; Shi, L.; Andriotis, O. G.; Gruber, P.; Markovic, M.; Thurner, P. J.; Ossipov, D.; Liska, R.; Ovsianikov, A. *Angew. Chem., Int. Ed.* **2018**, *57*, 15122−15127.
(43) Yu, Z.; Ohulchanskyy, T. Y.; An, P.; Prasad, P. N.; Lin, Q. *J. Am. Chem. Soc.* **2013**, *135*, 16766−16769.
(44) Shao, Y.; Zhao, J.; Yuan, J.; Zhao, Y.; Li, L. *Angew. Chem., Int. Ed.* **2021**, *60*, 8923−8931.
(45) Xie, S.; Du, Y.; Zhang, Y.; Wang, Z.; Zhang, D.; He, L.; Qiu, L.; Jiang, J.; Tan, W. *Nat. Commun.* **2020**, *11*, 1347.
(46) Zhang, X.-W.; Hatamie, A.; Ewing, A. G. *J. Am. Chem. Soc.* **2020**, *142*, 4093−4097.
(47) Wu, L.; Zhang, X.; Liu, W.; Xiong, E.; Chen, J. *Anal. Chem.* **2013**, *85*, 8397−8402.

https://doi.org/10.1021/acs.analchem.1c02049
Anal. Chem. 2021, 93, 11547−11556